Childs Nerv Syst (2018) 34:107–116
https://doi.org/10.1007/s00381-017-3633-5

ORIGINAL PAPER

Significance of H3K27M mutation with specific histomorphological features and associated molecular alterations in pediatric high-grade glial tumors

Süheyla Uyar Bozkurt[1] · A. Dagcinar[2] · B. Tanrikulu[3] · N. Comunoglu[4] · B. C. Meydan[5] · M. Ozek[3] · B. Oz[4]

Received: 8 June 2017 / Accepted: 16 October 2017 / Published online: 24 October 2017

Abstract
Purpose Pediatric high-grade gliomas (pHGGs) constitute almost 15% of all childhood brain tumors. Recurrent mutations such as H3K27M mutation in H3F3A and HIST1H3B genes encoding histone H3 and its variants were identified in approximately 30% of pediatric glioblastomas. This study aimed to ascertain the morphological and molecular characteristics of pHGGs with H3K27M mutation.
Methods In total, 61 cases of pHGGs (anaplastic astrocytoma, 12; glioblastomas, 49) from four university hospitals were studied. The histomorphological features were examined and immunohistochemistry was performed to evaluate the mutation status of H3K27M, ATRX, IDH1, BRAF V600E, and p53 genes.
Results The study comprised 25 females and 36 males (age range, 1–18 years) with a clinical follow-up of up to 108 months. From the total, 31 patients were positive for H3K27M mutation located in the midline, mostly in the pons and thalamus. H3K27M mutation was commonly associated with ATRX loss (32.3%) and p53 (74.2%) immunoreactivity with a co-expression rate of 25.8%. While IDH1 mutation was not detected in pHGGs with H3K27M mutation, BRAFV600E mutation was rarely observed. Among the various histomorphological features, increased number of mitosis, increased Ki-67 proliferation index, and palisading and geographical necrosis along with small cell patterns were significantly associated with the H3K27M wild-type tumors. Focal infarct-like necrosis and pilomyxoid morphology was significantly associated with these tumors.
Conclusion H3K27M mutation occurs exclusively in pHGGs arising from the midline and presents with varied histomorphological features ranging from low-grade pilomyxoid astrocytoma to highly pleomorphic glioblastoma along with ATRX loss and p53 mutations.

Keywords ATRX · p53 · Histomorphology · BRAF V600E

Introduction

Pediatric high-grade gliomas (pHGGs), including anaplastic astrocytoma (AA), diffuse intrinsic pontine glioma (DIPG), and glioblastoma (GBM), constitute almost 15% of all childhood tumors in the central nervous system (CNS) [1]. pHGGs are highly aggressive tumors that have led to an increase in childhood cancer mortality with no effective treatments available. Despite the similarities in the histopathology of these childhood and adult tumors, differences in behavior have been observed between the pediatric and adult patients. Furthermore, in spite of the poor prognosis of pediatric glioblastoma, the survival of pediatric patients is longer than that of the adults [2]. Integrated molecular genetic profiling showed significant differences in copy number alterations between childhood and adult GBM like PDGFRA amplification [3]. Recently, with the aid of genomic sequencing studies, recurrent mutations in H3F3A and HIST1H3B genes

✉ Süheyla Uyar Bozkurt
subozkurt@gmail.com;suheyla@marmara.edu.tr

[1] Department of Pathology, Marmara University Training and Research Hospital, Fevzi Cakmak Mah. Mimar Sinan Cad. No: 41 Ust Kaynarca Pendik, Istanbul, Turkey

[2] Department of Neurosurgery, Marmara University, Istanbul, Turkey

[3] Department of Neurosurgery, Acibadem University, Istanbul, Turkey

[4] Department of Pathology, Cerrahpasa Faculty, Istanbul University, Istanbul, Turkey

[5] Department of Pathology, Ondokuzmayis University, Samsun, Turkey

encoding histone H3 and variants were identified in approximately 30% of pediatric GBMs [4, 5] and 78% of DIPG [6]. Mutations in the H3F3A gene were detected at two positions: the lysine residue is replaced by methionine at position 27 (H3K27M mutation) and the glycine residue is replaced by arginine or valine at position 34 (H3G34R/V mutation) [4–7]. These mutations play a role in gliomagenesis by altering or interfering with the post translational modification sites for histones, which have a significant function in the regulation of gene expression [8]. Understanding the role of histone mutations in the pathogenesis of gliomas has highlighted the development of targeted therapies. Recently, reduced tumor cell viability and extended survival of mice with K27M mutant glioma xenografts were demonstrated via the inhibition of histone H3K27 demethylase by GSKJ4 [9]. In future, it is important to determine the occurrence of H3K27M mutations during treatment planning in high-grade glioma patients. Genomic studies in pHGGs have demonstrated additional mutations in H3K27 mutant gliomas, which include p53 and ATRX mutations [4, 7, 10], ACVR1 mutation, and receptor tyrosine kinase/RAS/PI3K mutations like PDGFR amplification and amplifications in cell cycle genes, such as CDK4/6 and CCND1 [11].

While H3K27M mutations have been reported in gliomas arising from midline locations, H3G34R/V mutations have been found in gliomas arising from the cerebral hemispheres [5–8, 12, 13]. Although H3K27M mutations in glial tumors were detected via sequencing-based studies, in recent years, it is possible to ascertain these tumors by immunohistochemical staining for anti-H3K27M antibodies with 100% sensitivity and specificity [14, 15].

The morphology of H3K27M mutant gliomas is varied; even in the absence of the histological features of high-grade glioma they are accepted as WHO grade IV [16]. Only a limited number of studies have evaluated the morphologic features of H3K27M-mutated gliomas [13, 17, 18]. One study reported a broad morphological spectrum in a sample involving all age groups [13]. In another study, a distinct histomorphology was reported among the molecular subtypes of glioblastoma in young patients under 30 years of age [17]. In the present study, we investigated the histomorphological features of HGGs focusing on the detection of the histomorphological characteristics and associated molecular alterations of H3K27M-mutated cases in pediatric patients.

Methods

In this retrospective study, 61 cases diagnosed as AA ($n = 12$) and GBM ($n = 49$) were examined. Formalin-fixed paraffin-embedded (FFPE) tumor tissues of patients who underwent stereotaxic biopsy ($n = 10$) or surgery ($n = 51$) were retrieved from the archives of the pathology laboratories of four university hospitals. Hematoxylin and eosin (H&E) stained original and newly cut sections were reviewed and the cases were classified according to the WHO classification of CNS tumors [16]. To evaluate tumor heterogeneity, each tumor was examined with at least two H&E sections at different levels. The study was approved by the ethics committees of the Marmara University (Protocol # 09.2016.598).

Immunohistochemistry

FFPE tissue sections (4 μm thick) were dried overnight at 37 °C and loaded onto a Ventana Benchmark Ultra Immunostainer (Roche Ventana Benchmark Ultra, Germany). The following primary antibodies were used for the immunohistochemical analyses: H3K27M mutant protein (1:200, #ABE419, Millipore, Billerica, MA, USA); BRAF V600E mutant protein (1:100, Clone VE1, #E19294, Spring Bioscience, Pleasanton, CA, USA); IDH1 R132H mutant protein (1:100, #H09, Dianova, Hamburg, Germany); ATRX (1:300, #sc-55,584, Santa Cruz Biotechnology, Texas, U.S.A.); Ki67 (1:100, MIB1, #M7240, Dako, Agilent Technologies, Glostrup, Denmark); and p53 (1:100, D-7, #MS-186-RQ Thermo Scientific, Fremont, USA). The positive controls included melanoma for BRAF V600E (known BRAF V600E mutation positive case), diffuse astrocytoma for IDH1 (known IDH1 mutation positive case), normal brain for ATRX, colon carcinoma for p53, and normal tonsil for ki67 according to manufacturer's instructions. Negative controls were used without application of the primary antibodies.

Evaluation of histomorphology

Histological features such as necrosis (palisading/geographical/ischemia-like focal), vascular endothelial cell proliferation, and microcalcification were considered as positive if observed in the tissues. The presence of mitosis was counted in 10 high power fields (hpf). Furthermore, the tissues were considered as positive for nuclear pleomorphism, epithelioid and small cell morphology, primitive neuroectodermal tumor (PNET)-like and microcystic areas, gemistocytic appearance with perivascular arrangement of the tumor cells when these characteristics were observed in more than 10% of the tumor area. Piloid and myxoid morphology, multinucleated giant cells and oligodendroglioma-like morphology were graded as 0 if absent or present in less than 10% of the tumor area, +1 when present in 10–30% of the tumor area, and +2 when present in more than 30% of the tumor area (Fig. 1a–c, e, h, i, k, l).

Evaluation of immunohistochemistry

Immunostaining for H3K27M was evaluated according to the nuclear staining of the tumor cells. The presence of nuclear staining for H3K27M mutant protein in the tumor cells but not

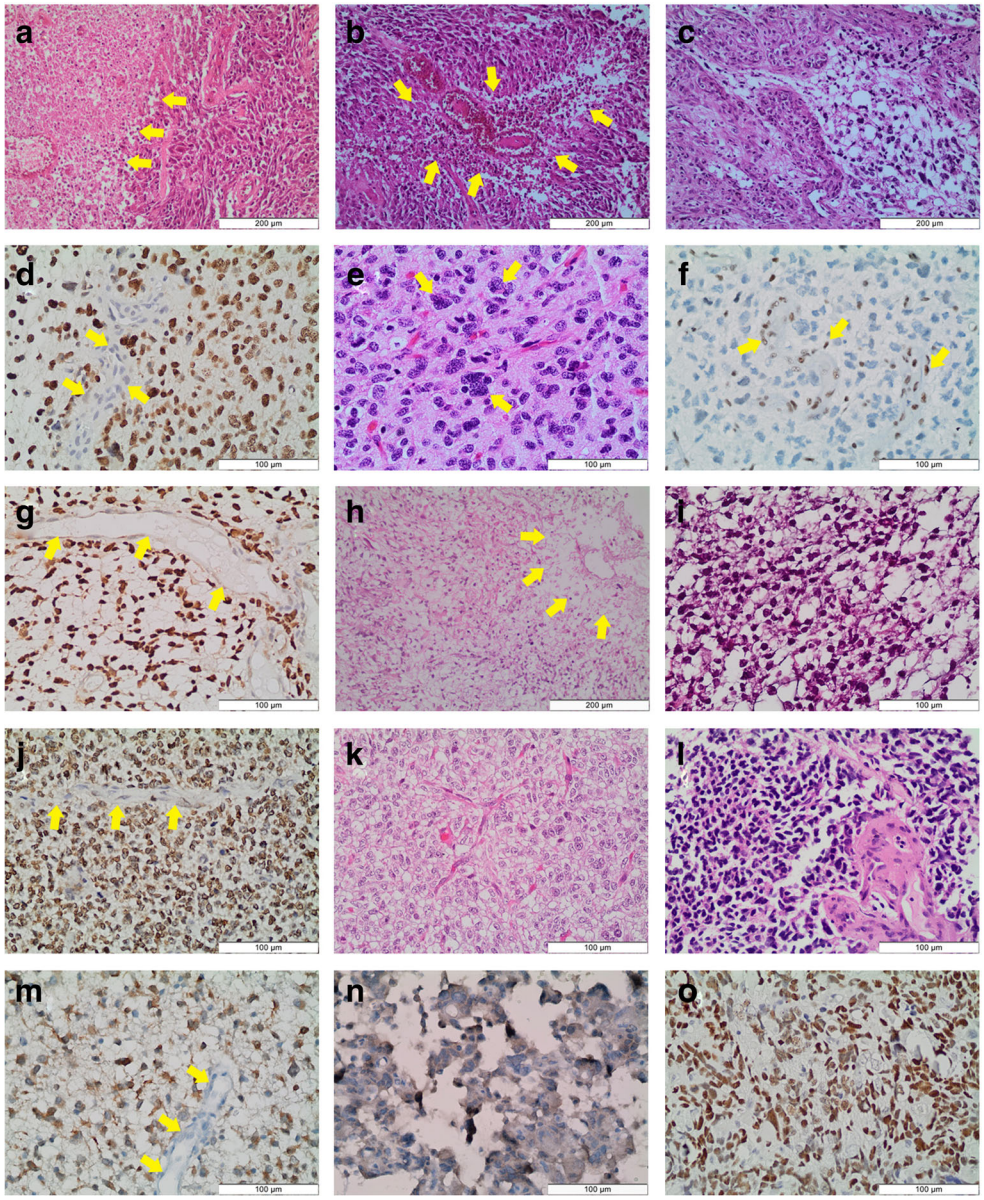

Fig. 1 Morphological and immunohistochemical features of pHGGs. **a** Geographical necrosis (arrows) (H&E, ×200). **b** Palisading necrosis (arrows) (H&E, ×200). **c** VEP (H&E, ×200). **d–f** H3K27M-mutated glioma with multinucleated giant cells. **d** Immunohistochemical expression of H3K27M mutant protein in tumor cells (arrows indicate endothelial cells) (H3K27M, ×400). **e** Pleomorphic and multinucleated tumor cells (arrows) (H&E, ×400). **f** Loss of immunohistochemical expression of ATRX in tumor cells (arrows indicate endothelial cells) (ATRX, ×400). **g–h** H3K27M-mutated glioma with pilocytic like morphology **g** Immunohistochemical expression of H3K27M mutant protein in tumor cells (arrows indicate endothelial cells) (H3K27M, ×400). **h** Pilocytic morphology and focal-ischemia-like necrosis (arrows) in tumor cells (H&E, ×200). **i** Myxoid morphology (H&E, ×400). **j–k** H3K27M-mutated glioma with oligodendroglioma-like appearance. **j** Immunohistochemical expression of H3K27M mutant protein in tumor cells (arrows indicate endothelial cells) (H3K27M, ×400). **k** Oligodendroglioma-like morphology (H&E, ×400). **l** Small cell morphology (H&E, ×400). **m** Immunohistochemical expression of IDH1 mutant protein in tumor cells (arrows indicate endothelial cells) (IDH1, ×400). **n** Immunohistochemical expression of BRAF V600E mutant protein in tumor cells (BRAF V600E, ×400). **o** The p53 immunoreactivity (graded as +3) in tumor cells (p53, ×400). Scale bar represent 200 μm ×200, 100 μm ×400 objectives

in the endothelial cells or normal brain was considered as evidence of mutation [14, 15]. Due to the difficulty in distinguishing non-specific cytoplasmic immunoreactivity in microglial/inflammatory cells, and necrosis, tumors that did not contain these areas were selected for evaluation by immunostaining. For ATRX, complete loss of nuclear staining in tumor cells with retained expression in the non-tumor cells was considered as loss of nuclear protein expression. For both IDH1 and BRAF V600E, diffuse cytoplasmic immunoreactivity was considered as evidence of mutation [19, 20]. p53

immunoreactivity was determined by approximation of the number of positively stained tumor cell nuclei in hpf (×400). p53 immunoreactivity was graded as 0 when no staining of the nuclei was observed; +1 when less than 10% of the nuclei were stained; +2 when 10–50% of the nuclei were stained; and +3 when more than 51% of the tumor cells nuclei were stained [21]. The Ki-67 proliferative index was expressed in percentage by determining the number of immunopositive nuclei calculated by manually counting 1000 nuclei in the area of maximal staining for each tumor in hpf (×400) [21] (Fig. 1d, f, g, j, m–o).

Statistical analysis

Statistical analysis was performed using SPSS 2015 Statistical Software program. Descriptive statistical methods (mean value, frequency tables, and standard deviation) were used. Differences between groups were ascertained by Pearson chi-square tests, T test, and Fisher's exact test. Cancer-specific survival outcome was expressed by applying the Kaplan-Meier method for all patients excluding those lost to follow-up. Log-rank test was used to compare the prognostic significance of H3K27M mutation on survival. Differences with a p value < 0.05 were considered statistically significant.

Results

Patients and follow-up

The present study included 61 patients: 25 females and 36 males. The mean age at diagnosis was 10.1 years (age range, 1–18 years). Of these, 12 (19.7%) patients had AA and 49 (80.3%) had GBMs. We also classified patients into two subgroups according to the H3K27M mutation status; 31 were positive for H3K27M mutation, and 30 were positive for the wild-type H3K27M mutation. The number of males was higher in the H3K27M wild-type group (female: male, 1:3.2), whereas in the H3K27M mutant group, females were more in number (1.3:1; Fisher's exact tests, $p < 0.05$). Among the pHGGs, 25 were located in the cerebral hemispheres, and 36 in the midline. All 25 cases arising from the cerebral hemisphere presented with wild type H3K27M mutation; 31 of the 36 cases arising from midline locations were positive for H3K27M mutation, while the remaining five presented with wild-type for H3K27M mutation. Among the HGGs arising from midline locations, 14 were located in the pons, 12 in the thalamus, seven in the cerebellum, two in the third ventricle, and one in the basal ganglia. A total of 43 patients had been treated with both chemotherapy and radiotherapy, and five patients had received radiotherapy only. Data from clinical follow-up of up to 108 months were obtained in 49 patients. The mean follow-up was 16.56 months (range, 2–108 months). During this period, 20 recurrences were detected in eight patients with H3K27M mutation and 12 patients with H3K27M wild-type gliomas. Of the 38 patients who died, 20 had the H3K27M mutant, and 18 had H3K27M wild-type gliomas. There were no significant differences in the recurrence rate and survival status between the patients presenting with H3K27M mutations and those with H3K27M wild-type gliomas (Fisher's exact tests, $p > 0.05$) (Table 1).

Among the 61 HGG cases, 31 were located in the midline locations and were positive for H3K27M; none of the cases located in the cerebral hemispheres was positive for H3K27M. Statistical analysis demonstrated a significant association between H3K27M mutations in the midline vs cerebral hemisphere locations ($p < 0.001$). Furthermore, in the midline sites, H3K27M mutation was most commonly seen in the pons (41.9%) and the thalamus (32.3%) (Table 1).

Association between histomorphological features and H3K27M status

The mean number of mitosis was 4.3 in H3K27M-mutated and 11.2 in H3K27M wild-type gliomas. Statistical analysis demonstrated a significant association between the number of mitosis and H3K27M mutation status ($p < 0.01$). In addition, the mean Ki-67 proliferation indexes were 28.9% for H3K27M-mutated, and 41.5% for H3K27M wild-type gliomas ($p < 0.05$). When types of necrosis were examined, palisading and geographical necrosis were mostly seen in H3K27M wild-type gliomas; infarct-like focal necrosis was frequently observed in the H3K27M-mutated cases ($p < 0.05$). Pleomorphism of the tumor cells was the most commonly encountered morphological feature followed by multinucleated giant cells in both H3K27M-mutated and wild-type gliomas. Pilocytic morphology representing elongated tumor cells and myxoid morphology characterized by mucinous areas between tumor cells were significantly more common in H3K27M-mutated gliomas ($p < 0.01$). The pilomyxoid areas were seen in more than 30% (+2) of the tumor areas in majority of the H3K27M-mutated gliomas (51.6% cases). Piloid morphology was most commonly detected in tumors that presented with midline H3K27M-mutated HGGs located in the pons (12/13 pontine cases; $p < 0.05$). Small cell morphology, characterized by monomorphic small, round cells, was mostly seen in H3K27M wild-type gliomas ($p < 0.05$). In this study, some of the morphological features such as vascular endothelial cell proliferation, epithelioid-like appearance in tumor cells, primitive PNET-like foci, gemistocytic appearance in tumor cells, perivascular arrangement of tumor cells, and microcalcification were more frequently noted in the H3K27M wild-type gliomas. Alternatively, multinucleated giant tumor cells, clear haloes giving an oligodendroglioma-like appearance to tumor cells, and microcystic areas were more frequently observed in the

Table 1 Clinicopathologic features of pHGGs according to Histone H3K27M mutation status

	H3K27M positive	H3K27M negative	Total
Number of patients	31	30	61
Sex			
Male	13	23	36
Female	18	7	25
Age			
Mean ± SD	9.2 ± 3.8	11.1 ± 4.8	
Tumor type			
Anaplastic astrocytoma	10	2	12
Glioblastoma	21	28	49
Location			
Cerebral hemispheres	0	25	25
Midline location	31	5	36
Pons	13	1	14
Thalamus	10	2	12
Cerebellum	5	2	7
Third ventricle	2	0	2
Basal ganglia	1	0	1
Radiotherapy			
Positive	24	24	48
Negative	2	2	4
Unknown	5	4	9
Chemotherapy			
Positive	19	24	43
Negative	7	2	9
Unknown	5	4	9
Recurrence status			
Positive	8	12	20
Negative	17	13	30
Unknown	6	5	11
Survival status			
Alive	5	6	11
Exitus	20	18	38
Unknown	6	6	12

SD standard deviation

H3K27M-mutated gliomas. However, no statistical association was elucidated among these morphological features and mutation status ($p > 0.05$; Table 2).

Association between molecular alterations and H3K27M status

Table 2 shows the immunohistochemical results of ATRX, IDH1R132H, BRAF-V600E and p53 staining in H3K27M mutant and wild-type pHGGs. ATRX loss was revealed in 10 of the H3K27M-mutated (32.3%), and five of the wild-type gliomas (16.7%) cases. It was mostly seen in tumors arising from the thalamus 40% (4/10) and pons 23.1% (3/13) in H3K27M-mutated group. IDH1R132H positivity was only seen in one H3K27M wild-type glioma case located in the cerebral hemisphere; this case also showed both ATRX loss and p53 immunopositivity. BRAF-V600E positivity was revealed in four cases with three in the H3K27M mutant, and one in the H3K27M wild-type gliomas. p53 immunopositivity was seen in 74.2% of the H3K27M-mutated and 63.3% of the wild-type gliomas. Majority of these cases expressed p53 positivity in > 50% of the tumor cells (+3 expression score). No statistically significant differences in immunohistochemical results of ATRX, IDH1R132H, BRAF V600E, and p53 was found between the H3K27M-mutated and wild-type gliomas ($p > 0.05$; Table 2).

Table 2 Frequency of molecular alterations and histomorphological features of pHGGs according to H3K27M mutation status

	H3-K27M positive (n = 31) (%)	H3-K27M negative (n = 30)(%)	p value
Molecular alterations			
ATRX[1]			
Loss	10(32.3)	5(16.7)	>0.05
Sustained	21(67.7)	25(83.3)	
IDH1-R132H[1]			
Positive	0(0)	1(3.3)	>0.05
Negative	31(100)	29(96.7)	
BRAF-V600E[1]			
Positive	3(9.7)	1(3.3)	>0.05
Negative	28(90.3)	29(96.7)	
P53 expression score[2]			
0	8(25.8)	11(36.7)	>0.05
+1	1(3.2)	2(6.7)	
+2	7(22.6)	5(16.7)	
+3	15(48.4)	12(40.0)	
Histomorphological features			
Mitosis[3]			
Mean ± SD	4.3 ± 4.2	11.2 ± 9.8	**0.001**[4]
Ki-67 PI[3]			
Mean ± SD	28.2 ± 18.5	41.4 ± 20.6	**0.01**[4]
Palisading necrosis[1]	6(19.4)	14(46.7)	**<0.05**[4]
Geographic necrosis[1]	5(16.1)	14(46.7)	**<0.05**[4]
Ischemia-like focal necrosis[1]	11(35.5)	3(10.0)	**<0.05**[4]
Vascular endothelial proliferation (VEP)[1]	15(48.4)	17(56.7)	>0.05
Pleomorphism[1]	27(87.1)	29(96.7)	>0.05
Epithelioid-like morphology[1]	3(9.7)	6(20.0)	>0.05
PNET-like morphology[1]	0(0)	2(6.7)	>0.05
Small cell morphology[1]	3(9.7)	12(40.0)	**<0.05**[4]
Gemistocytic morphology[1]	4(12.9)	8(26.7)	>0.05
Microcystic morphology[1]	14(45.2)	6(20.0)	>0.05
Perivascular arrangement[1]	9(29.0)	10(33.3)	>0.05
Microcalcification[1]	3(9.7)	4(13.3)	>0.05
Multinucleated giant cell[2]			
0	10(32.3)	14(46.7)	>0.05
+1	10(32.3)	4(13.3)	
+2	11(35.5)	12(40.0)	
Pilocytic morphology[2]			
0	7(22.6)	26(86.7)	**0.001**[4]
+1	8(25.8)	3(10.0)	
+2	16(51.6)	1(3.3)	
Myxoid morphology[2]			
0	8(25.8)	25(83.3)	**0.001**[4]
+1	7(22.6)	4(13.3)	
+2	16(51.6)	1(3.3)	
Oligodendroglioma-like morphology[2]			
0	16(48.4)	20(66.7)	>0.05
+1	11(35.5)	7(23.3)	
+2	5(16.1)	3(10.0)	

SD standard deviation

[1] Fisher's Exact test

[2] Pearson chi-square test

[3] T-test

[4] Significant p value <0.05 (determined separately for mitosis, Ki 67 proliferation indexes, all types of necrosis, small cell morphology, pilocytic morphology, myxoid morphology between H3K27M mutated vs H3K27M wild-type of pHGGs)

There were overlapping molecular alterations in 25.8% (8/31) of the H3K27M-mutated cases. Both p53 immunoreactivity and ATRX loss were mostly found in the thalamus (4/8) and pons (2/8). p53 and ATRX co-expressions were found in 10% (3/30) of the H3K27M wild-type cases, one of which demonstrated the co-expression of IDH1, p53, and ATRX. No concomitant IDH1 and H3K27M mutation was found (Fig. 2).

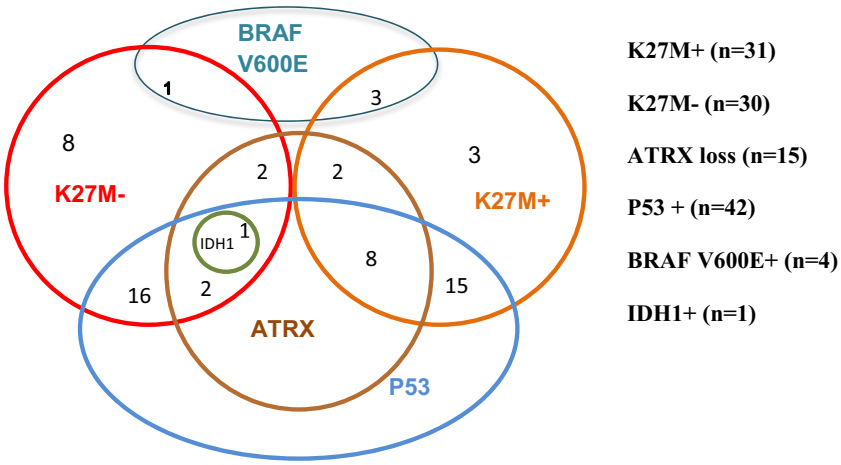

Fig. 2 Schematic presentation of the overlapping mutations in the pHGGs

Association between H3K27M status and survival

The median overall survival period of HGG patients was 15 months; median overall survival period of H3K27M-mutated patients was 12 months, and wild-type H3K27M tumor patients was 17 months. Although overall survival was lower in the H3K27M-mutated group, the difference was not statistically significant (Log-rank test, $p > 0.05$).

Discussion

Molecular studies of pHGGs identified recurrent somatic mutations in the H3F3A gene encoding histone H3, and in HIST1H3B and HIST1H3C genes encoding histone H3.1, thereby affecting a region of posttranslational modification [22]. One of these recurrent somatic mutations, H3K27M mutation, results in the substitution of H3 lysine 27 to methionine, which occurs in 78% of DIPG and almost 30% of pediatric glioblastoma [4, 6, 10, 17, 23, 24]. The present study revealed the highest number of H3K27M mutations (50.8%) in pHGGs when compared with previous studies in the literature [4, 10, 17, 23, 24]. This may be due to a sample bias because half of the patients in this study presented with tumors located in the midline. Although H3K27M-mutant pHGGs have been reported to have no significant sex predilection, in the present study, a female predominance was observed [16].

H3K27M mutation leads to a decrease in H3 with trimethylated lysine 27 (H3K27me3) by inhibiting the enzymatic activity of the Polycomb repressive complex 2 (PRC2), which contains the EZH2 (enhancer of zeste) K27 methyltransferase, resulting in epigenetic silencing and promotion of gliomagenesis [25–27]. Additionally, it is reported that global hypomethylation of DNA induced by K27M mutation plays a role in the expression of genes in pHGGs [27]. Jha et al. demonstrated the involvement of pathways regulating neuron differentiation, neuron fate commitment, and neurogenesis in H3F3A K27M-mutant tumors [28]. Inhibition of PRC2 also contributes to the progression of neural precursor cell differentiation due to the disappearance of its suppressor role in neuronal differentiation [29].

The present study revealed H3K27M mutations exclusively in midline locations in the thalamus, pons, cerebellum, third ventricle, and basal ganglia, as reported in the literature [7, 13, 18]. Among the midline sites, this mutation was found mostly in pons and thalamus in our study. It is suggested that the location specification of histone mutation is related to the different origins or the developmental stages of the cells in high-grade gliomas [7]. Gene expression signatures of K27M mutant gliomas were found to be associated with the mid to late fetal stages of striatal and thalamic development [7].

Currently, WHO has classified infiltrative high-grade gliomas with predominantly astrocytic differentiation in midline locations and harboring K27M mutation in either H3F3A or HIST1H3B/C genes as diffuse midline glioma, H3K27M mutant [16]. The morphology of these gliomas is varied; even in the absence of the histological features of high-grade gliomas, they are accepted as grade IV. Solomon et al. reported a wide morphological spectrum including giant cells, epithelioid and rhabdoid cells, PNET-like foci, pilomyxoid features, ependymal and pleomorphic xanthoastrocytoma-like areas, sarcomatous transformation, and ganglionic differentiation in H3K27M-mutated diffuse midline glioma patients aged 2–65 years old [13]. In the present study, the principal morphological criteria of HGGs, which include mitosis, necrosis, vascular endothelial cell proliferation, and the various morphological patterns seen in glial tumors, were assessed in H3K27M-mutated and wild-type pHGGs. Nuclear pleomorphism and multinucleated giant cells were the frequently observed morphologic features in both types of gliomas. Increased numbers of mitosis, with pronounced palisading and geographical necrosis, and small cell patterns were significantly more common in the H3K27M wild-type tumors; meanwhile, focal infarct-like necrosis and pilomyxoid morphology were significantly associated with the H3K27M-mutated tumors. This low-grade pilomyxoid morphology can be confusing during differential

diagnosis with pilocytic astrocytoma. The distinction is important especially in cases of limited tumor sample size obtained by stereotactic biopsy. Piloid morphology was significantly more common in tumors located in the pons among the midline H3K27M-mutated HGGs. The Ki67 proliferation indices were significantly higher in H3K27M wild-type tumors. Multinucleated giant cells, oligodendroglioma-like appearance, and microcystic areas were also more commonly seen in H3K27M-mutated tumors, statistical significance notwithstanding. Neumann et al. reported that K27M-mutated glioblastomas had 28% tumor giant cells [17]. It was also suggested that, phenotypical features of the K27M-mutated tumors were correlated with the types of genes involved in the mutation [30]. Castel et al. defined the two subgroups of DIPG according to the genes involved in K27M mutation as H3F3A and HIST1H3A, which were associated with the proneural/oligodendroglial phenotype and the mesenchymal/astrocytic phenotype, respectively [30]. PNET-like areas was the only histological parameter that was not seen in H3K27M-mutated pHGGs in the current study. Although, PNET-like foci has been reported in H3K27M-mutated tumors [13], this morphology was significantly defined in the H3F3A G34R-mutated glioblastomas [17]. Furthermore, when the relationship between the location and morphological appearance of the tumors was investigated in all pHGGs, significant associations were found between pilomyxoid and small cell morphology, which were significantly more common in the pons and cerebral hemispheres, respectively.

Histone H3.3 acts as a replacement histone and is expressed throughout the cell cycle [22]. DNA synthesis independent H3.3 is mainly found in the telomeric and pericentric heterochromatin, and their incorporation into these areas is accomplished by the ATRX-DAXX (alpha thalassemia/mental retardation syndrome X-linked and death-domain associated protein) chromatin remodeling complex [8, 22, 31]. ATRX loss has been shown to be associated with the alternative lengthening of telomeres (ALT) in pancreatic neuroendocrine tumors, pediatric and adult GBMs [4, 32]. In the present study, approximately one third of the H3K27M-mutated pHGGs showed ATRX loss, which is consistent with the literature [4, 10, 17]. Schwartzentruber et al. reported that the presence of ALT was best explained by the simultaneous presence of ATRX/H3F3A/TP53 mutations in pediatric GBMs [4]. In fact, ATRX mutation also has been reported frequently in H3G34-mutated HGGs [4, 10, 17, 33]. To prevent the possible misinterpretation of H3G34-mutated HGGs as H3K27M wild-type, it would be worthwhile to investigate the relationship between the H3G34 mutation and the ATRX mutation in H3K27M wild-type cases.

The results of the current study showed p53 mutation in 68% of all pHGGs with similar frequencies in the H3K27M-mutated and wild-type gliomas. Eight of the H3K27M-mutated patients also showed ATRX loss and p53 immunoreactivity with predilection to the thalamus. The results of our study suggest that H3K27M mutation in combination with ATRX loss and p53 mutation play a role in the pathogenesis of pHGGs.

Mutations in genes coding the mitochondrial enzymes isocitrate dehydrogenase 1 (IDH1) and 2 have been reported in approximately 80% of adult diffuse and anaplastic gliomas and secondary glioblastoma [34]. Zhang et al. reported IDH1 mutations in 16.8% of young adult glioblastoma patients with favorable prognosis [35]. Although these mutations are rarely seen in pediatric gliomas [3, 34], favorable prognosis was also reported in IDH1-mutant pediatric glioblastomas [36, 37]. In the present study, only one pHGG was positive for the IDH1-R132H-mutant protein. No concomitant mutation of IDH1 and H3K27M was found supporting the suggestion that H3K27M mutation is mutually exclusive from IDH1 mutation [7, 13, 17, 35, 36].

The association between BRAF V600E and H3K27M mutations has recently been reported in midline gliomas [11, 13, 17, 38, 39]. Glioneuronal [38] and pleomorphic xanthoastrocytoma-like morphology [13] as well as intermediate prognosis [38, 39] were noticed in these concomitantly mutated gliomas. In our study, three patients showed concomitant BRAF V600E and H3K27M mutant protein expression. Although double mutation is rare, its prognostic significance should be evaluated in larger number of samples.

The prognostic significance of molecular alterations in pHGGs has been suggested in several studies; in particularly, the presence of H3K27M mutation has been associated with poor prognosis when compared with the wild-type variants [12, 36, 40, 41]. In the present study, although, the median overall survival was lower in the H3K27M-mutated patients when compared with those having the wild-type tumors, statistical significance notwithstanding. Interestingly, although patients H3K27M-mutated tumors presented with lower mitosis and Ki67 proliferation index and with low-grade pilomyxoid-like morphology, they had a shorter median overall survival period than those with the wild-type tumors, which is contrary to the better clinical behavior expected. This may be due to the fact that all H3K27M-mutated tumors are located in the midline with spreading pathways that pass through vital areas such as the pons and medulla oblongata; hence, complete surgical resection is difficult. In this study, there were no significant differences in recurrence rate and survival status between H3K27M mutant and wild-type pHGGs. However, it should be noted that disparate treatment modalities resulting from the inclusion of cases from different institutions limit our recurrence and survival analyses.

Conclusion

H3K27M mutation occurs exclusively in pHGGs arising from the midline and presenting with varied histomorphological

findings extending from low-grade pilomyxoid astrocytoma to highly pleomorphic glioblastoma. Although the steps involved in the gliomagenesis of H3K27M-mutated pHGGs remains unclear, ATRX loss and p53 mutations may play a role in the pathogenesis. Being aware of these molecular alterations can lead to the development of new targeted therapies in patients with dismal prognosis.

Acknowledgments The authors thank Gülcan Davulcu for secretarial assistance, Demet Bayrak, Ardınç Arpınar, for laboratory support, and Prof. Nural Bekiroğlu for statistical analysis.

Compliance with ethical standards

Conflict of interest On behalf of all authors, the corresponding author states that there is no conflict of interest.

References

1. Ostrom QT, Gittleman H, Fulop J, Liu M, Blanda R, Kromer C, Wolinsky Y, Kruchko C, Barnholtz-Sloan JS (2015) CBTRUS statistical report: primary brain and central nervous system tumors diagnosed in the United States in 2008–2012. Neuro Oncol 17 Suppl 4:iv1–iv62
2. Das KK, Mehrotra A, Nair AP, Kumar S, Srivastava AK, Sahu RN, Kumar R (2012) Pediatric glioblastoma: clinico-radiological profile and factors affecting the outcome. Childs Nerv Syst 28:2055–2062
3. Paugh BS, Qu C, Jones C, Liu Z, Adamowicz-Brice M, Zhang J, Bax DA, Coyle B, Barrow J, Hargrave D, Lowe J, Gajjar A, Zhao W, Broniscer A, Ellison DW, Grundy RG, Baker SJ (2010) Integrated molecular genetic profiling of pediatric high-grade gliomas reveals key differences with the adult disease. J Clin Oncol 28: 3061–3068
4. Schwartzentruber J, Korshunov A, Liu XY, Jones DT, Pfaff E, Jacob K, Sturm D, Fontebasso AM, Quang DA, Tönjes M, Hovestadt V, Albrecht S, Kool M, Nantel A, Konermann C, Lindroth A, Jäger N, Rausch T, Ryzhova M, Korbel JO, Hielscher T, Hauser P, Garami M, Klekner A, Bognar L, Ebinger M, Schuhmann MU, Scheurlen W, Pekrun A, Frühwald MC, Roggendorf W, Kramm C, Dürken M, Atkinson J, Lepage P, Montpetit A, Zakrzewska M, Zakrzewski K, Liberski PP, Dong Z, Siegel P, Kulozik AE, Zapatka M, Guha A, Malkin D, Felsberg J, Reifenberger G, von Deimling A, Ichimura K, Collins VP, Witt H, Milde T, Witt O, Zhang C, Castelo-Branco P, Lichter P, Faury D, Tabori U, Plass C, Majewski J, Pfister SM, Jabado N (2012) Driver mutations in histone H3.3 and chromatin remodelling genes in paediatric glioblastoma. Nature 482:226–231
5. Rheinbay E, Louis DN, Bernstein BE, Suvà ML (2012) A tell-tail sign of chromatin: histone mutations drive pediatric glioblastoma. Cancer Cell 21:329–331
6. Wu G, Broniscer A, TA ME, Lu C, Paugh BS, Becksfort J, Qu C, Ding L, Huether R, Parker M, Zhang J, Gajjar A, Dyer MA, Mullighan CG, Gilbertson RJ, Mardis ER, Wilson RK, Downing JR, Ellison DW, Baker SJ, Project SJCsRHWUPCG (2012) Somatic histone H3 alterations in pediatric diffuse intrinsic pontine gliomas and non-brainstem glioblastomas. Nat Genet 44:251–253
7. Sturm D, Witt H, Hovestadt V, Khuong-Quang DA, Jones DT, Konermann C, Pfaff E, Tönjes M, Sill M, Bender S, Kool M, Zapatka M, Becker N, Zucknick M, Hielscher T, Liu XY, Fontebasso AM, Ryzhova M, Albrecht S, Jacob K, Wolter M, Ebinger M, Schuhmann MU, van Meter T, Frühwald MC, Hauch H, Pekrun A, Radlwimmer B, Niehues T, von Komorowski G, Dürken M, Kulozik AE, Madden J, Donson A, Foreman NK, Drissi R, Fouladi M, Scheurlen W, von Deimling A, Monoranu C, Roggendorf W, Herold-Mende C, Unterberg A, Kramm CM, Felsberg J, Hartmann C, Wiestler B, Wick W, Milde T, Witt O, Lindroth AM, Schwartzentruber J, Faury D, Fleming A, Zakrzewska M, Liberski PP, Zakrzewski K, Hauser P, Garami M, Klekner A, Bognar L, Morrissy S, Cavalli F, Taylor MD, van Sluis P, Koster J, Versteeg R, Volckmann R, Mikkelsen T, Aldape K, Reifenberger G, Collins VP, Majewski J, Korshunov A, Lichter P, Plass C, Jabado N, Pfister SM (2012) Hotspot mutations in H3F3A and IDH1 define distinct epigenetic and biological subgroups of glioblastoma. Cancer Cell 22:425–437
8. Lee J, Solomon DA, Tihan T (2017) The role of histone modifications and telomere alterations in the pathogenesis of diffuse gliomas in adults and children. J Neuro-Oncol 132:1–11
9. Hashizume R, Andor N, Ihara Y, Lerner R, Gan H, Chen X, Fang D, Huang X, Tom MW, Ngo V, Solomon D, Mueller S, Paris PL, Zhang Z, Petritsch C, Gupta N, Waldman TA, James CD (2014) Pharmacologic inhibition of histone demethylation as a therapy for pediatric brainstem glioma. Nat Med 20:1394–1396
10. Pathak P, Jha P, Purkait S, Sharma V, Suri V, Sharma MC, Faruq M, Suri A, Sarkar C (2015) Altered global histone-trimethylation code and H3F3A-ATRX mutation in pediatric GBM. J Neuro-Oncol 121:489–497
11. Wu G, Diaz AK, Paugh BS, Rankin SL, Ju B, Li Y, Zhu X, Qu C, Chen X, Zhang J, Easton J, Edmonson M, Ma X, Lu C, Nagahawatte P, Hedlund E, Rusch M, Pounds S, Lin T, Onar-Thomas A, Huether R, Kriwacki R, Parker M, Gupta P, Becksfort J, Wei L, Mulder HL, Boggs K, Vadodaria B, Yergeau D, Russell JC, Ochoa K, Fulton RS, Fulton LL, Jones C, Boop FA, Broniscer A, Wetmore C, Gajjar A, Ding L, Mardis ER, Wilson RK, Taylor MR, Downing JR, Ellison DW, Baker SJ, Project SJCRHWUPCG (2014) The genomic landscape of diffuse intrinsic pontine glioma and pediatric non-brainstem high-grade glioma. Nat Genet 46:444–450
12. Khuong-Quang DA, Buczkowicz P, Rakopoulos P, Liu XY, Fontebasso AM, Bouffet E, Bartels U, Albrecht S, Schwartzentruber J, Letourneau L, Bourgey M, Bourque G, Montpetit A, Bourret G, Lepage P, Fleming A, Lichter P, Kool M, von Deimling A, Sturm D, Korshunov A, Faury D, Jones DT, Majewski J, Pfister SM, Jabado N, Hawkins C (2012) K27M mutation in histone H3.3 defines clinically and biologically distinct subgroups of pediatric diffuse intrinsic pontine gliomas. Acta Neuropathol 124:439–447
13. Solomon DA, Wood MD, Tihan T, Bollen AW, Gupta N, Phillips JJ, Perry A (2015) Diffuse midline gliomas with histone H3-K27M mutation: a series of 47 cases assessing the spectrum of morphologic variation and associated genetic alterations. Brain Pathol
14. Venneti S, Santi M, Felicella MM, Yarilin D, Phillips JJ, Sullivan LM, Martinez D, Perry A, Lewis PW, Thompson CB, Judkins AR (2014) A sensitive and specific histopathologic prognostic marker for H3F3A K27M mutant pediatric glioblastomas. Acta Neuropathol 128:743–753
15. Bechet D, Gielen GG, Korshunov A, Pfister SM, Rousso C, Faury D, Fiset PO, Benlimane N, Lewis PW, Lu C, David Allis C, Kieran MW, Ligon KL, Pietsch T, Ellezam B, Albrecht S, Jabado N (2014) Specific detection of methionine 27 mutation in histone 3 variants (H3K27M) in fixed tissue from high-grade astrocytomas. Acta Neuropathol 128:733–741
16. Louis DN, Ohgaki H, Wiestler OD, Cavenee WK, Ellison DW, Figarella-Branger D, Perry A, Reifenberger G, Von Deimling A (2016) WHO classification of tumours of the central nervous system. IARC, Lyon
17. Neumann JE, Dorostkar MM, Korshunov A, Mawrin C, Koch A, Giese A, Schüller U (2016) Distinct histomorphology in molecular

subgroups of glioblastomas in young patients. J Neuropathol Exp Neurol 75:408–414
18. Ryall S, Krishnatry R, Arnoldo A, Buczkowicz P, Mistry M, Siddaway R, Ling C, Pajovic S, Yu M, Rubin JB, Hukin J, Steinbok P, Bartels U, Bouffet E, Tabori U, Hawkins C (2016) Targeted detection of genetic alterations reveal the prognostic impact of H3K27M and MAPK pathway aberrations in paediatric thalamic glioma. Acta Neuropathol Commun 4:93
19. Capper D, Weissert S, Balss J, Habel A, Meyer J, Jäger D, Ackermann U, Tessmer C, Korshunov A, Zentgraf H, Hartmann C, von Deimling A (2010) Characterization of R132H mutation-specific IDH1 antibody binding in brain tumors. Brain Pathol 20: 245–254
20. Kleinschmidt-DeMasters BK, Aisner DL, Foreman NK (2015) BRAF VE1 immunoreactivity patterns in epithelioid glioblastomas positive for BRAF V600E mutation. Am J Surg Pathol 39:528–540
21. Bozkurt SU, Ayan E, Bolukbasi F, Elmaci I, Pamir N, Sav A (2009) Immunohistochemical expression of SPARC is correlated with recurrence, survival and malignant potential in meningiomas. APMIS 117:651–659
22. Kallappagoudar S, Yadav RK, Lowe BR, Partridge JF (2015) Histone H3 mutations—a special role for H3.3 in tumorigenesis? Chromosoma 124:177–189
23. Gessi M, Gielen GH, Hammes J, Dörner E, Mühlen AZ, Waha A, Pietsch T (2013) H3.3 G34R mutations in pediatric primitive neuroectodermal tumors of central nervous system (CNS-PNET) and pediatric glioblastomas: possible diagnostic and therapeutic implications? J Neuro-Oncol 112:67–72
24. Gielen GH, Gessi M, Hammes J, Kramm CM, Waha A, Pietsch T (2013) H3F3A K27M mutation in pediatric CNS tumors: a marker for diffuse high-grade astrocytomas. Am J Clin Pathol 139:345–349
25. Lewis PW, Müller MM, Koletsky MS, Cordero F, Lin S, Banaszynski LA, Garcia BA, Muir TW, Becher OJ, Allis CD (2013) Inhibition of PRC2 activity by a gain-of-function H3 mutation found in pediatric glioblastoma. Science 340:857–861
26. Venneti S, Garimella MT, Sullivan LM, Martinez D, Huse JT, Heguy A, Santi M, Thompson CB, Judkins AR (2013) Evaluation of histone 3 lysine 27 trimethylation (H3K27me3) and enhancer of Zest 2 (EZH2) in pediatric glial and glioneuronal tumors shows decreased H3K27me3 in H3F3A K27M mutant glioblastomas. Brain Pathol 23:558–564
27. Bender S, Tang Y, Lindroth AM, Hovestadt V, Jones DT, Kool M, Zapatka M, Northcott PA, Sturm D, Wang W, Radlwimmer B, Højfeldt JW, Truffaux N, Castel D, Schubert S, Ryzhova M, Seker-Cin H, Gronych J, Johann PD, Stark S, Meyer J, Milde T, Schuhmann M, Ebinger M, Monoranu CM, Ponnuswami A, Chen S, Jones C, Witt O, Collins VP, von Deimling A, Jabado N, Puget S, Grill J, Helin K, Korshunov A, Lichter P, Monje M, Plass C, Cho YJ, Pfister SM (2013) Reduced H3K27me3 and DNA hypomethylation are major drivers of gene expression in K27M mutant pediatric high-grade gliomas. Cancer Cell 24:660–672
28. Jha P, Pia Patric IR, Shukla S, Pathak P, Pal J, Sharma V, Thinagararanjan S, Santosh V, Suri V, Sharma MC, Arivazhagan A, Suri A, Gupta D, Somasundaram K, Sarkar C (2014) Genome-wide methylation profiling identifies an essential role of reactive oxygen species in pediatric glioblastoma multiforme and validates a methylome specific for H3 histone family 3A with absence of G-CIMP/isocitrate dehydrogenase 1 mutation. Neuro-Oncology 16: 1607–1617
29. Hirabayashi Y, Suzki N, Tsuboi M, Endo TA, Toyoda T, Shinga J, Koseki H, Vidal M, Gotoh Y (2009) Polycomb limits the neurogenic competence of neural precursor cells to promote astrogenic fate transition. Neuron 63:600–613
30. Castel D, Philippe C, Calmon R, Le Dret L, Truffaux N, Boddaert N, Pagès M, Taylor KR, Saulnier P, Lacroix L, Mackay A, Jones C, Sainte-Rose C, Blauwblomme T, Andreiuolo F, Puget S, Grill J, Varlet P, Debily MA (2015) Histone H3F3A and HIST1H3B K27M mutations define two subgroups of diffuse intrinsic pontine gliomas with different prognosis and phenotypes. Acta Neuropathol 130:815–827
31. Lewis PW, Elsaesser SJ, Noh KM, Stadler SC, Allis CD (2010) Daxx is an H3.3-specific histone chaperone and cooperates with ATRX in replication-independent chromatin assembly at telomeres. Proc Natl Acad Sci U S A 107:14075–14080
32. Heaphy CM, de Wilde RF, Jiao Y, Klein AP, Edil BH, Shi C, Bettegowda C, Rodriguez FJ, Eberhart CG, Hebbar S, Offerhaus GJ, McLendon R, Rasheed BA, He Y, Yan H, Bigner DD, Oba-Shinjo SM, Marie SK, Riggins GJ, Kinzler KW, Vogelstein B, Hruban RH, Maitra A, Papadopoulos N, Meeker AK (2011) Altered telomeres in tumors with ATRX and DAXX mutations. Science 333:425
33. Sturm D, Pfister SM, Jones DTW (2017) Pediatric gliomas: current concepts on diagnosis, biology, and clinical management. J Clin Oncol 35:2370–2377
34. Yan H, Parsons DW, Jin G, McLendon R, Rasheed BA, Yuan W, Kos I, Batinic-Haberle I, Jones S, Riggins GJ, Friedman H, Friedman A, Reardon D, Herndon J, Kinzler KW, Velculescu VE, Vogelstein B, Bigner DD (2009) IDH1 and IDH2 mutations in gliomas. N Engl J Med 360:765–773
35. Zhang RQ, Shi Z, Chen H, Chung NY, Yin Z, Li KK, Chan DT, Poon WS, Wu J, Zhou L, Chan AK, Mao Y, Ng HK (2016) Biomarker-based prognostic stratification of young adult glioblastoma. Oncotarget 7:5030–5041
36. Korshunov A, Ryzhova M, Hovestadt V, Bender S, Sturm D, Capper D, Meyer J, Schrimpf D, Kool M, Northcott PA, Zheludkova O, Milde T, Witt O, Kulozik AE, Reifenberger G, Jabado N, Perry A, Lichter P, von Deimling A, Pfister SM, Jones DT (2015) Integrated analysis of pediatric glioblastoma reveals a subset of biologically favorable tumors with associated molecular prognostic markers. Acta Neuropathol 129:669–678
37. Korshunov A, Schrimpf D, Ryzhova M, Sturm D, Chavez L, Hovestadt V, Sharma T, Habel A, Burford A, Jones C, Zheludkova O, Kumirova E, Kramm CM, Golanov A, Capper D, von Deimling A, Pfister SM, Jones DT (2017) H3-/IDH-wild type pediatric glioblastoma is comprised of molecularly and prognostically distinct subtypes with associated oncogenic drivers. Acta Neuropathol
38. Nguyen AT, Colin C, Nanni-Metellus I, Padovani L, Maurage CA, Varlet P, Miquel C, Uro-Coste E, Godfraind C, Lechapt-Zalcman E, Labrousse F, Gauchotte G, Silva K, Jouvet A, Figarella-Branger D, Network FG (2015) Evidence for BRAF V600E and H3F3A K27M double mutations in paediatric glial and glioneuronal tumours. Neuropathol Appl Neurobiol 41:403–408
39. Zhang J, Wu G, Miller CP, Tatevossian RG, Dalton JD, Tang B, Orisme W, Punchihewa C, Parker M, Qaddoumi I, Boop FA, Lu C, Kandoth C, Ding L, Lee R, Huether R, Chen X, Hedlund E, Nagahawatte P, Rusch M, Boggs K, Cheng J, Becksfort J, Ma J, Song G, Li Y, Wei L, Wang J, Shurtleff S, Easton J, Zhao D, Fulton RS, Fulton LL, Dooling DJ, Vadodaria B, Mulder HL, Tang C, Ochoa K, Mullighan CG, Gajjar A, Kriwacki R, Sheer D, Gilbertson RJ, Mardis ER, Wilson RK, Downing JR, Baker SJ, Ellison DW, Project SJCRHWUPCG (2013) Whole-genome sequencing identifies genetic alterations in pediatric low-grade gliomas. Nat Genet 45:602–612
40. Buczkowicz P, Bartels U, Bouffet E, Becher O, Hawkins C (2014) Histopathological spectrum of paediatric diffuse intrinsic pontine glioma: diagnostic and therapeutic implications. Acta Neuropathol 128:573–581
41. Rizzo D, Ruggiero A, Martini M, Rizzo V, Maurizi P, Riccardi R (2015) Molecular biology in pediatric high-grade glioma: impact on prognosis and treatment. Biomed Res Int 2015:215135